Supplementary Information

Synthesis of Schiff bases of 2-amino benzo[d]thiazole from higher hetero aldehydes and ketones using Mo-Al_2O_3 composite-based organocatalyst

Koteswara Rao Anam & Ganesamoorthy Thirunarayanan*

Department of Chemistry, Annamalai University, Annamalainagar-608 002, India

*E-mail: drgtnarayanan@gmail.com; thirunarayanan.g.10313@annamalaiuniversity.ac.in

Received 5 August 2022; accepted (revised) 16 January 2023

Preparation of Mo-Al_2O_3 composite

About 20 ml of ethanol was taken in a conical flask in which (5 mmol, 0.98 g) $(NH_4)_2MoO_3$was added and sonicated up to colloidal suspension. In another conical flask 20 ml of ethanol which contains (5 mmol, 0.51 g) basic alumina (Al_2O_3) added and sonicated up to colloidal suspension, then the two solutions were added drop wise using separating funnel and stirred up to homogeneous mixture using a magnetic stirrer for 24 h. After the Mo-Al_2O_3 composites were formed then, the mixture was sonicated to get a fine power. The resulting solution was stirred for 4 h at room temperature. The solution was filtered with Buckner funnel using Whatmann filter paper at room temperature. The obtained solid was dried at 110°C for 5 h in oven and grind with a pestle and mortar affords the Mo-Al_2O_3 composites as fine powder. This catalyst was calcined at 400°C for 2h using muffle furnace. The obtained Mo-Al_2O_3 composite was characterized by the powder XRD (X-Ray Diffraction), SEM (Scanning Electron Microscopy), and EDS (Energy Dispersive X-ray Spectroscopy) analysis.

Catalyst characterization

FT-IR Analysis

The functional group assessment of the synthesized catalyst was characterised through FT-IR spectra. (Fig. S1) shows the FT-IR spectra of the synthesized ***Mo-Al_2O_3 composites.*** From the FT-IR spectrum, it could be determining that the absorption peak at 985 cm^{-1} was the stretching vibration of the 'O' double bond and the peaks at 878 cm^{-1}, 814 cm^{-1} and 673 cm^{-1} are due to the stretching vibrations of the Mo–O–Mo bond. The stretching vibration peak of the Al–O bond of the alumina, observed at 867 cm^{-1} and the bending vibrations of the bond was observed near 650 cm^{-1}. These observations indicate that Mo was well dispersed on the surface of the Al_2O_3 and metal-oxygen first-overtones were observed in the region of (2150-1850 cm^{-1}). Within this observations, the FT-IR results were in great agreement with XRD.

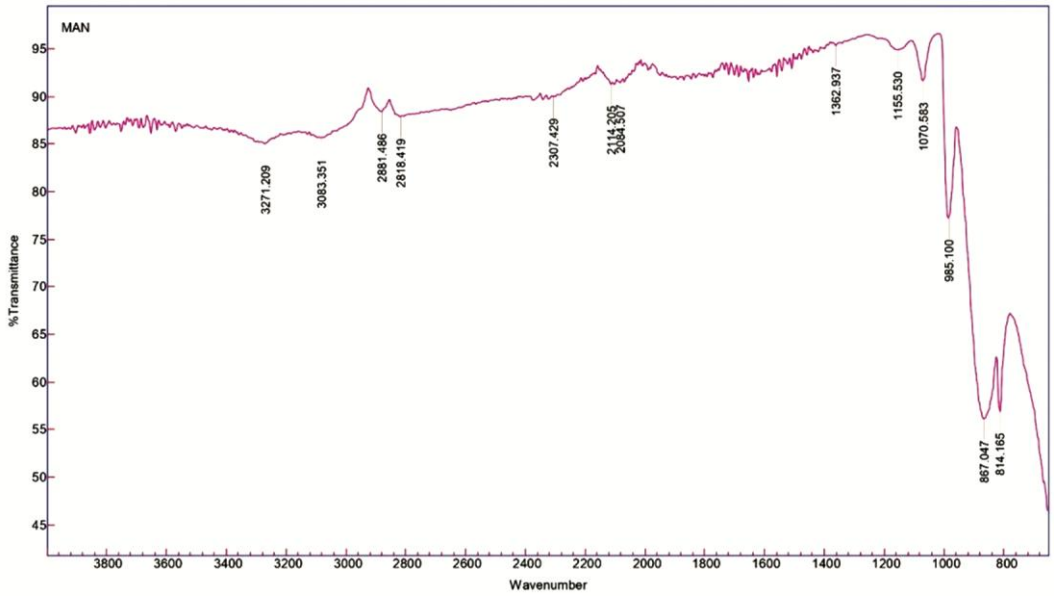

Fig. S1 — FTIR spectrumof Mo-Al_2O_3 composite

XRD analysis

Fig. S2 shows the Powder XRD pattern of synthesized composites**.** *The phase and crystalline nature of the prepared material was scrutinized by XRD analysis.* From the XRD spectra the diffraction peaks at $2\theta = 26.90^0$, 38.40^0 and 54.80^0 are corresponding to the Al_2O_3. They are nearly same to the characteristic diffraction peaks ofhierarchicallystructured Mo-Al_2O_3 catalyst. Moreover, the diffraction peaks are appeared in the well intense form indicating the crystallite nature of the sample**.** In addition, the characteristic peaks of molybdenum oxide were not obvious, indicating that molybdenum was uniformly dispersed inside and, on the alumina, and no agglomeration of oxides was formed, which coming from the synthesis of hierarchically macro-mesoporous Al_2O_3 supports. These composites are earlier reported by R. Torrecillas[23] at 450^0C. The XRD is closely matching with their patterns.

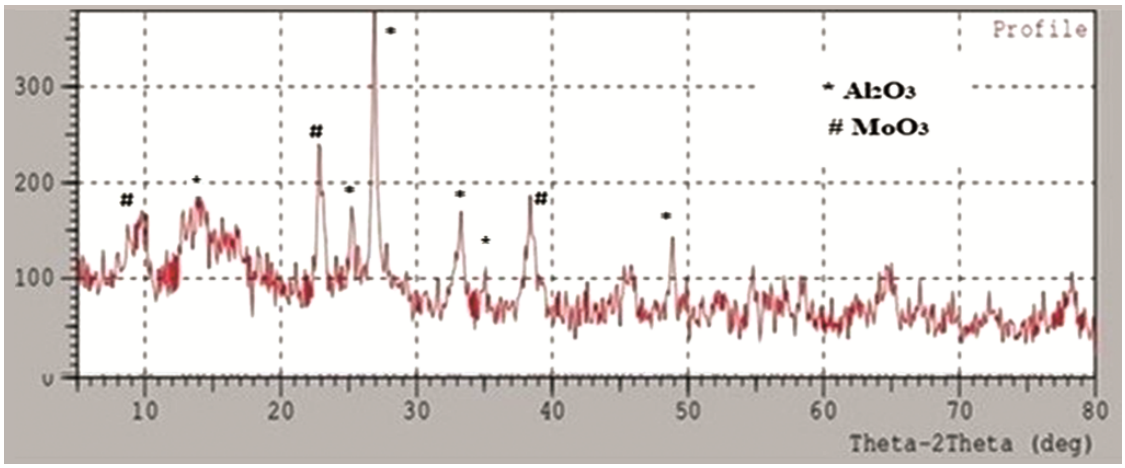

Fig. S2 — PXRD pattern of Mo-Al_2O_3 composites

SEM and EDX Analysis

The SEM images of the Mo-Al_2O_3 composites in Fig. S3 (a-b) displays surfaces of the catalyst particles. The Surface texture of the synthesized Mo-Al_2O_3 composite was analysed by SEM analysis. Fig. S3a shows the low magnification SEM image of catalyst, it shows the spherical shape of the prepared sample. Also the high magnification image (S3b) of the prepared catalyst shows the most of the particles are appeared in the form of flakes like structure. Moreover, the catalyst shows the less agglomeration, which is related to the better catalyst performance. In Energy Dispersion X-ray (EDS) analysis was performed for the Mo-Al_2O_3 composites which confirmed the presence of Mo, Al and O respective metal ions as shown in Fig. S3(c).

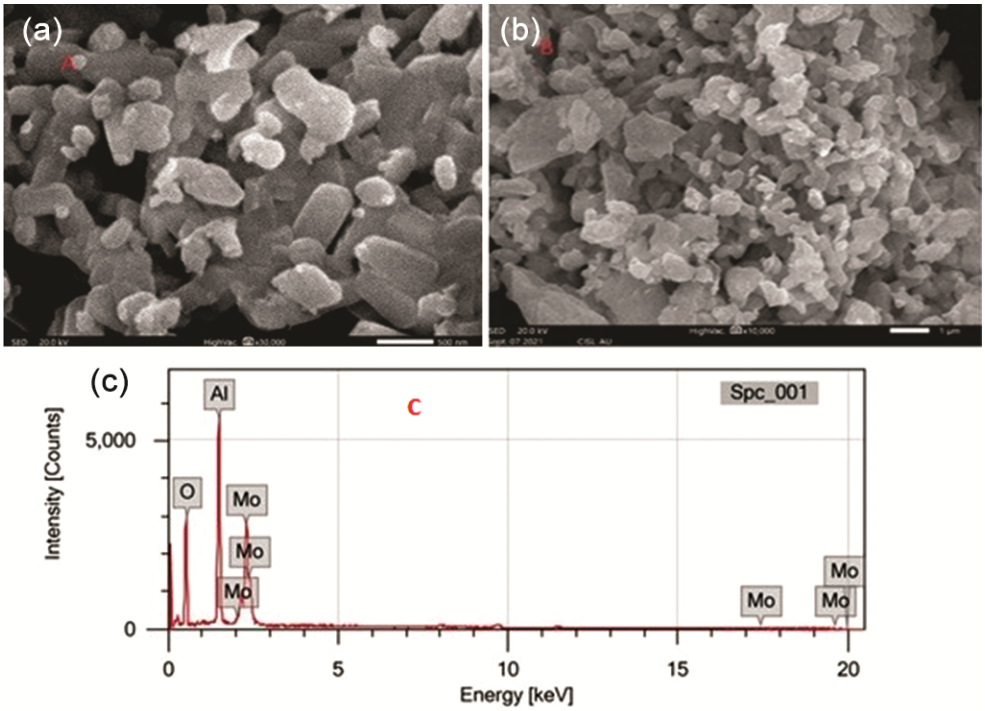

Fig. S3 — SEM images of Mo-Al_2O_3 composites at (a) scale-500 nm and (b) scale-1µm and (c) EDX image of Mo-Al_2O_3 composites

Reference

[23]. L.A. Diaz, A.F. Valdes, C. Diaz, A.M. Espino, R. Torrecillas, Alumina/molybdenum nanocomposites obtained in organic media, J. Eur. Ceram. Soc. 23 (2003) 2829–2834.

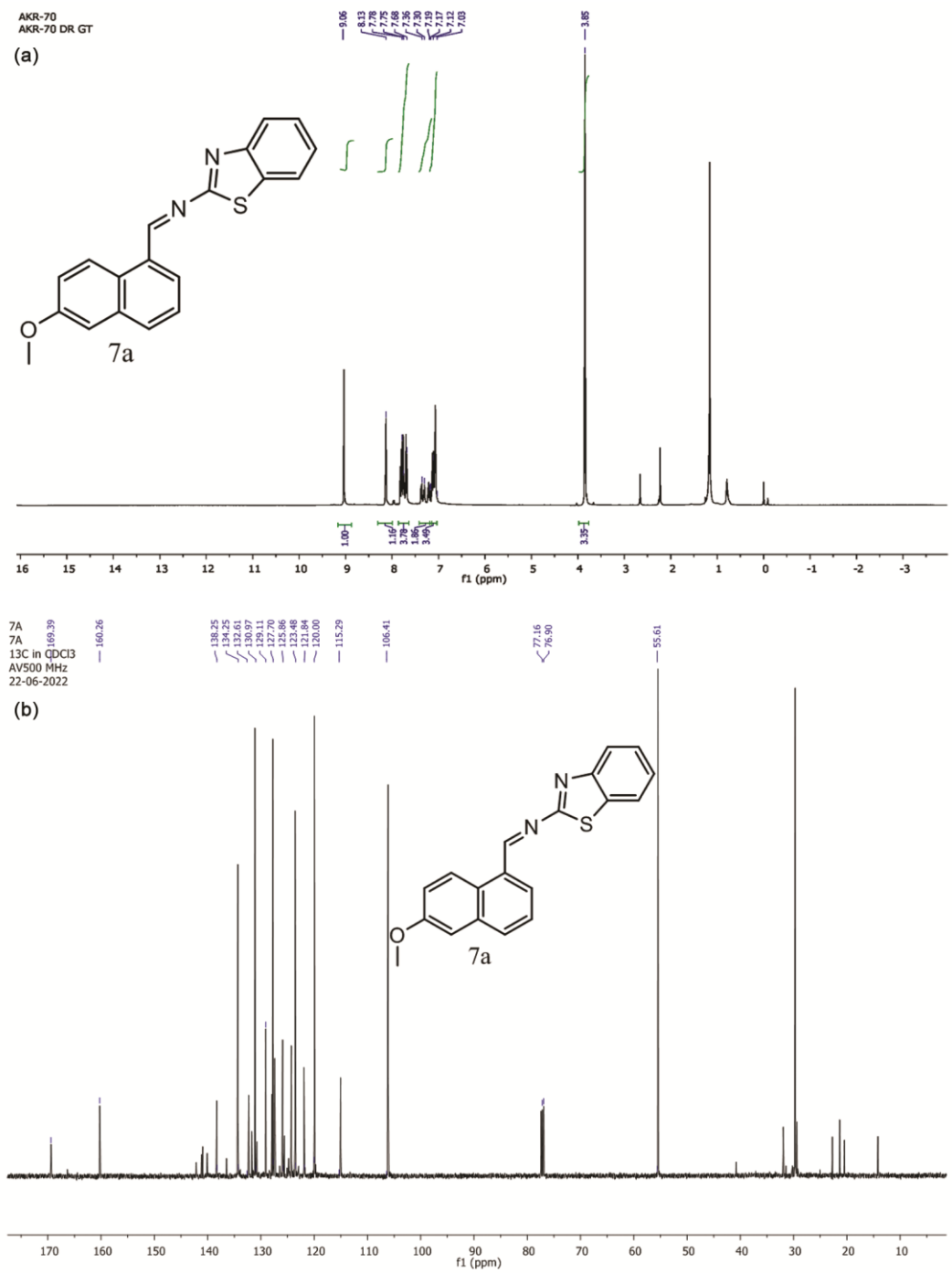

Fig. S4 — (a) ^{1}H and (b) C NMR spectra of compound 7a

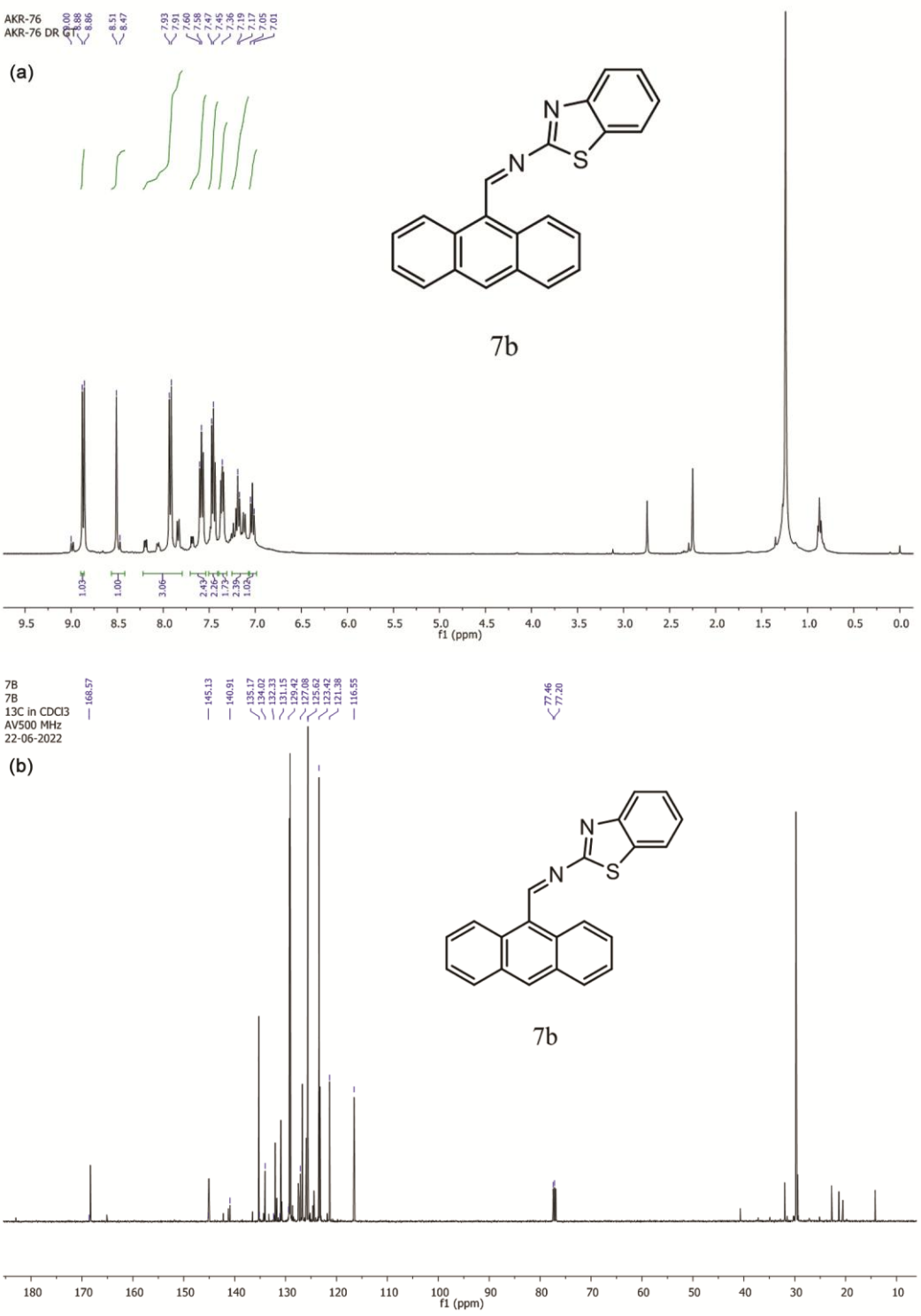

Fig. S5 — (a) ^{1}H and (b) C NMR spectra of compound 7b

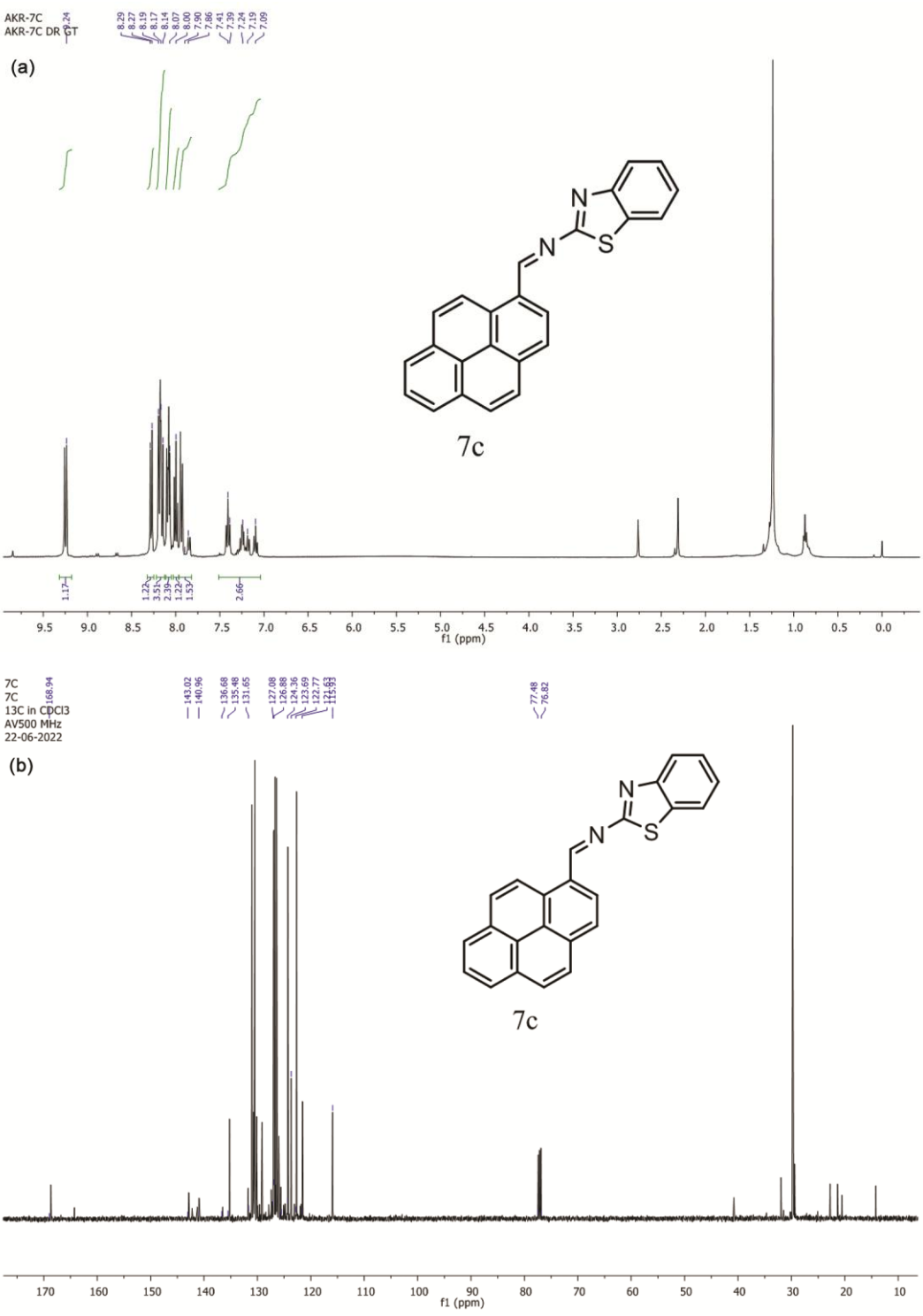

Fig. S6 — (a) ^{1}H and (b) C NMR spectra of compound 7c

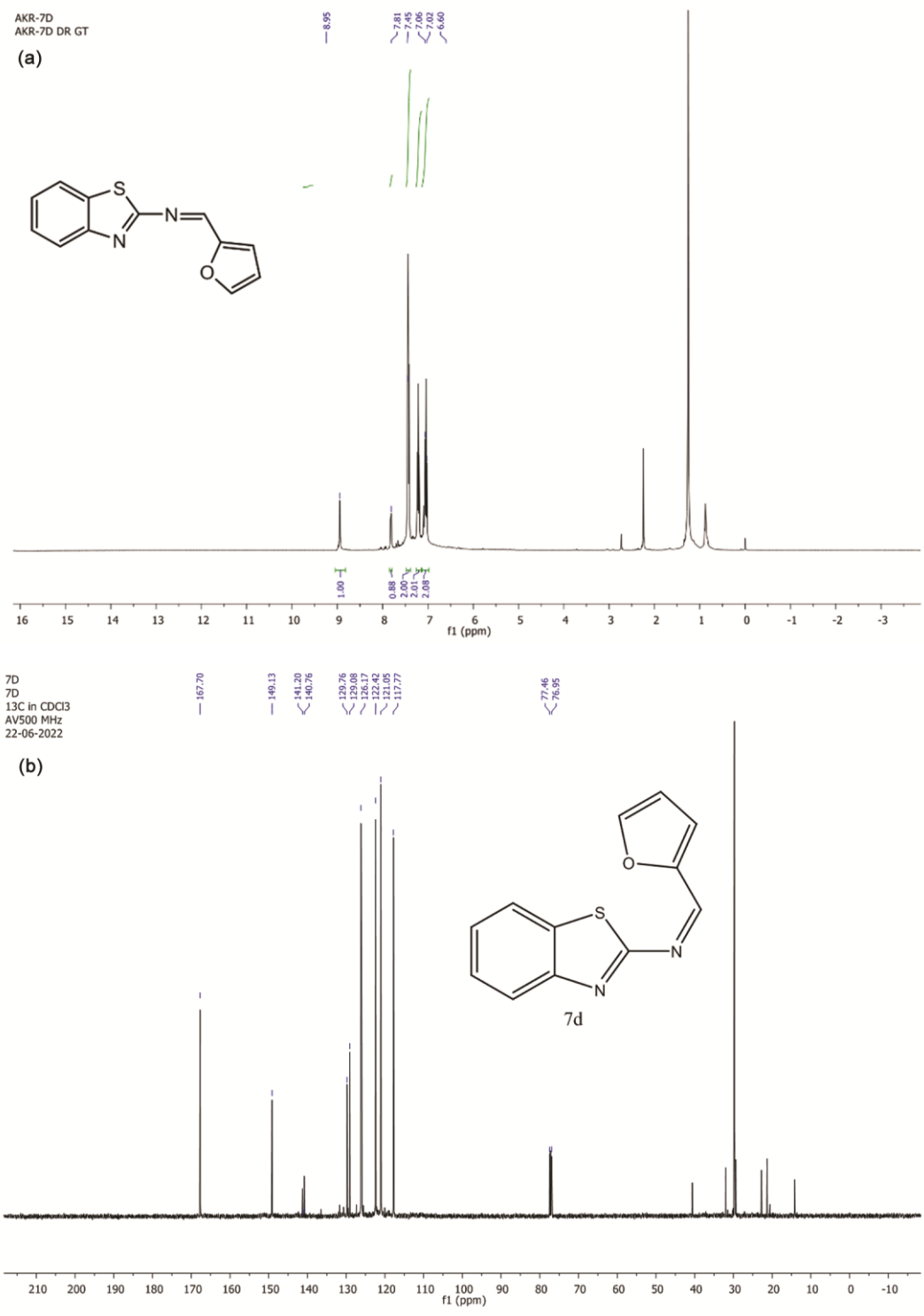

Fig. S7 — (a) ^{1}H and (b) C NMR spectra of compound 7d

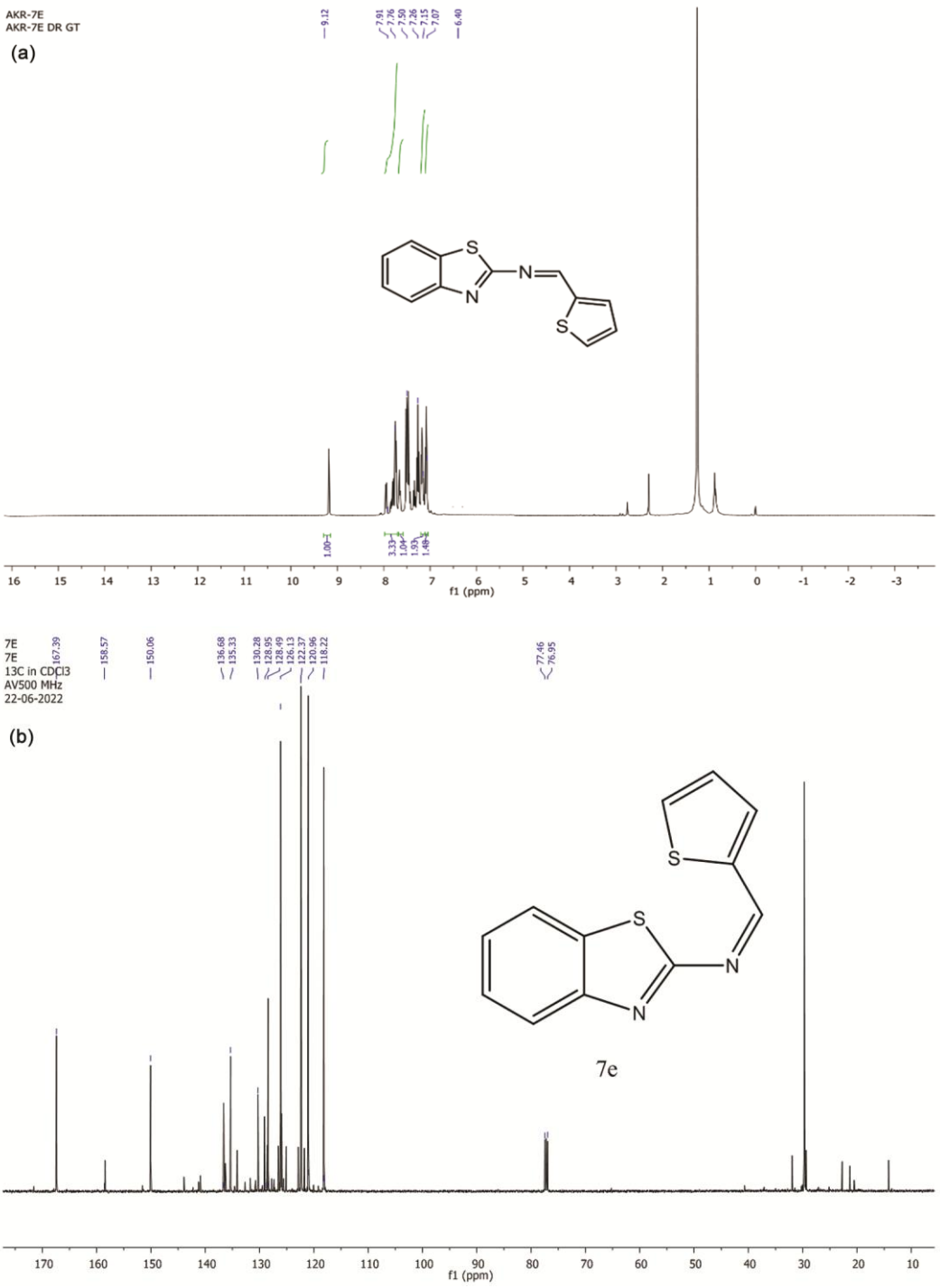

Fig. S8 — (a) ^{1}H and (b) C NMR spectra of compound 7e

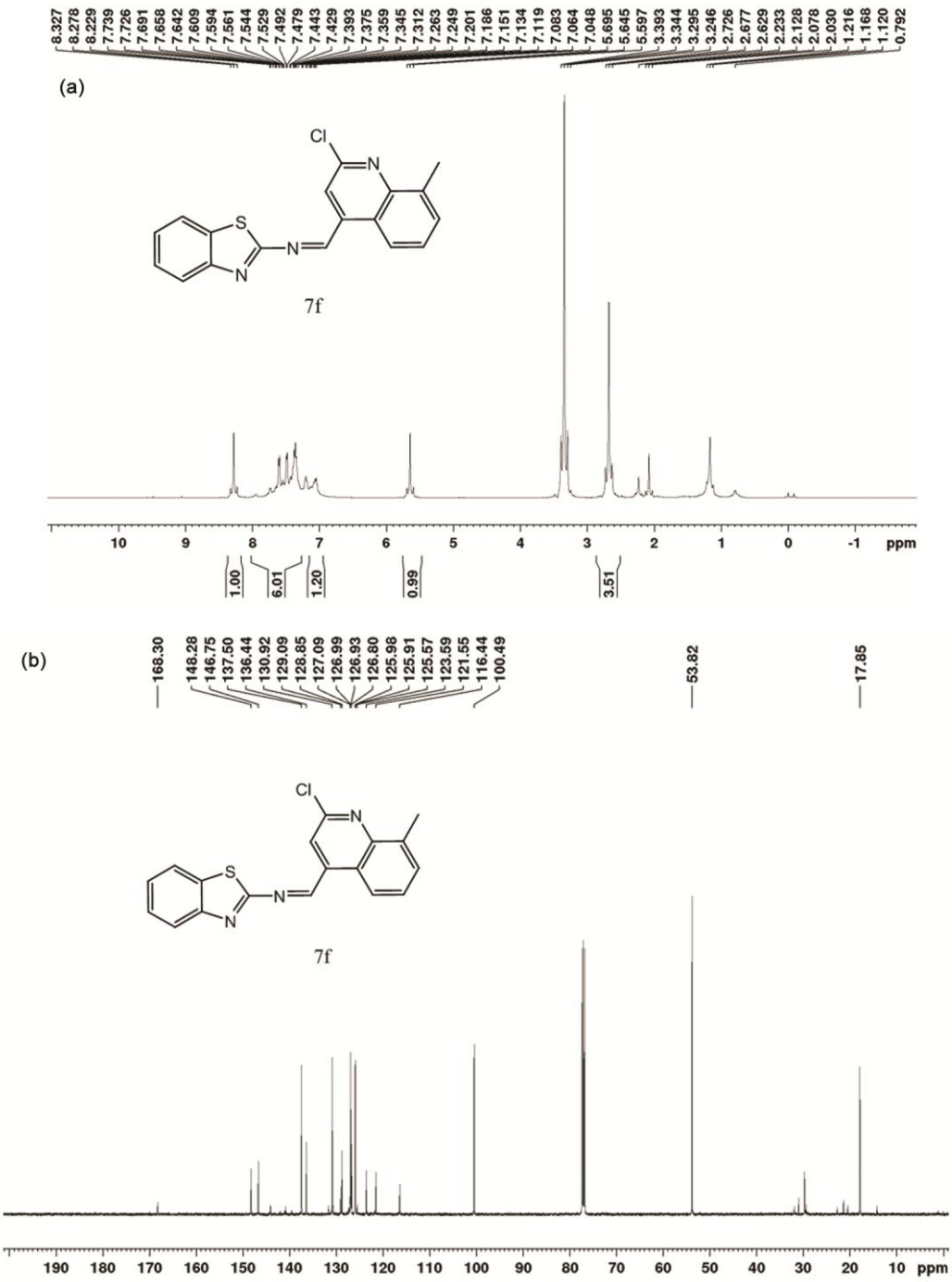

Fig. S9 — (a) ^{1}H and (b) C NMR spectra of compound 7f

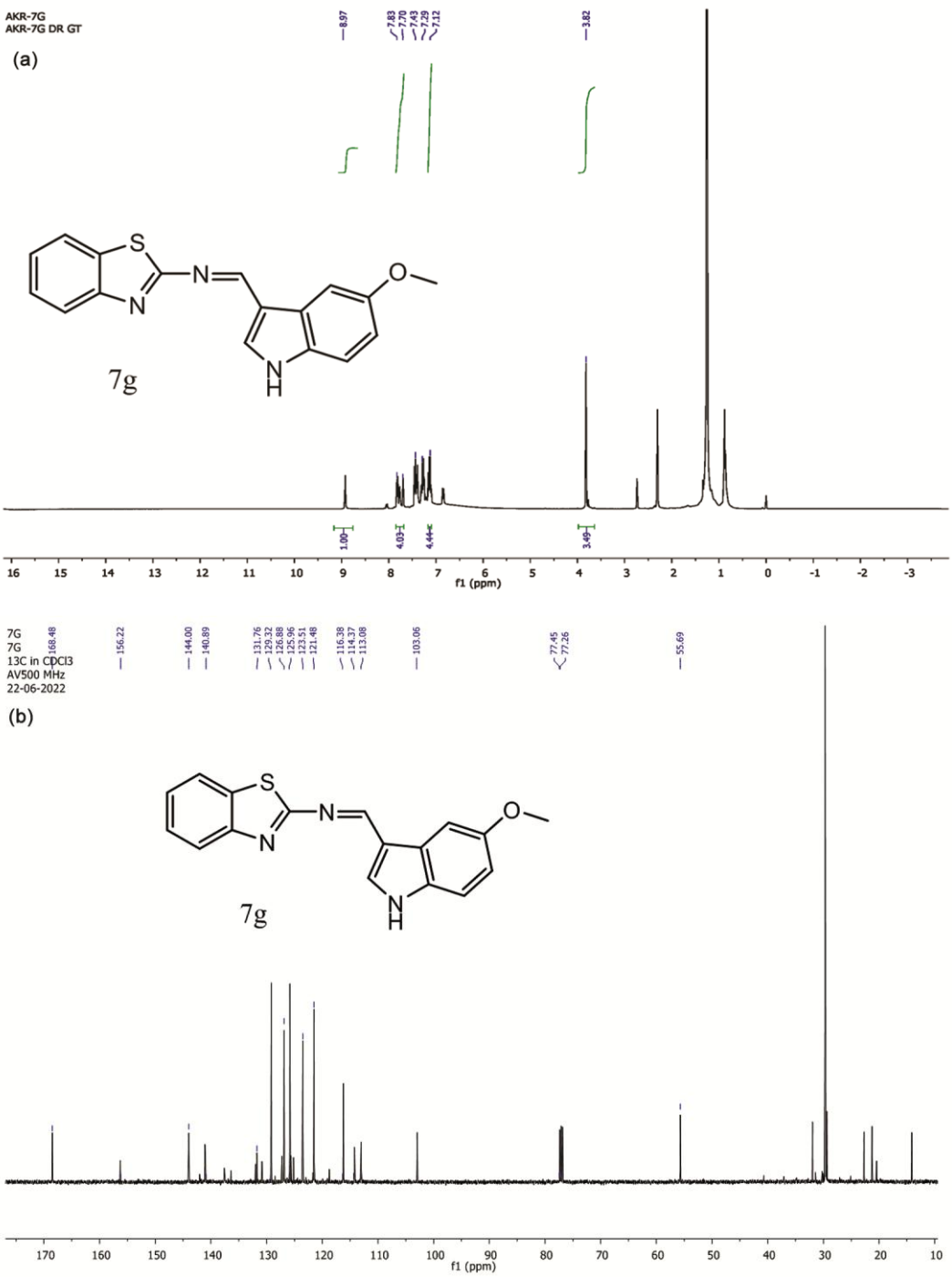

Fig. S10 — (a) ^{1}H and (b) C NMR spectra of compound 7g

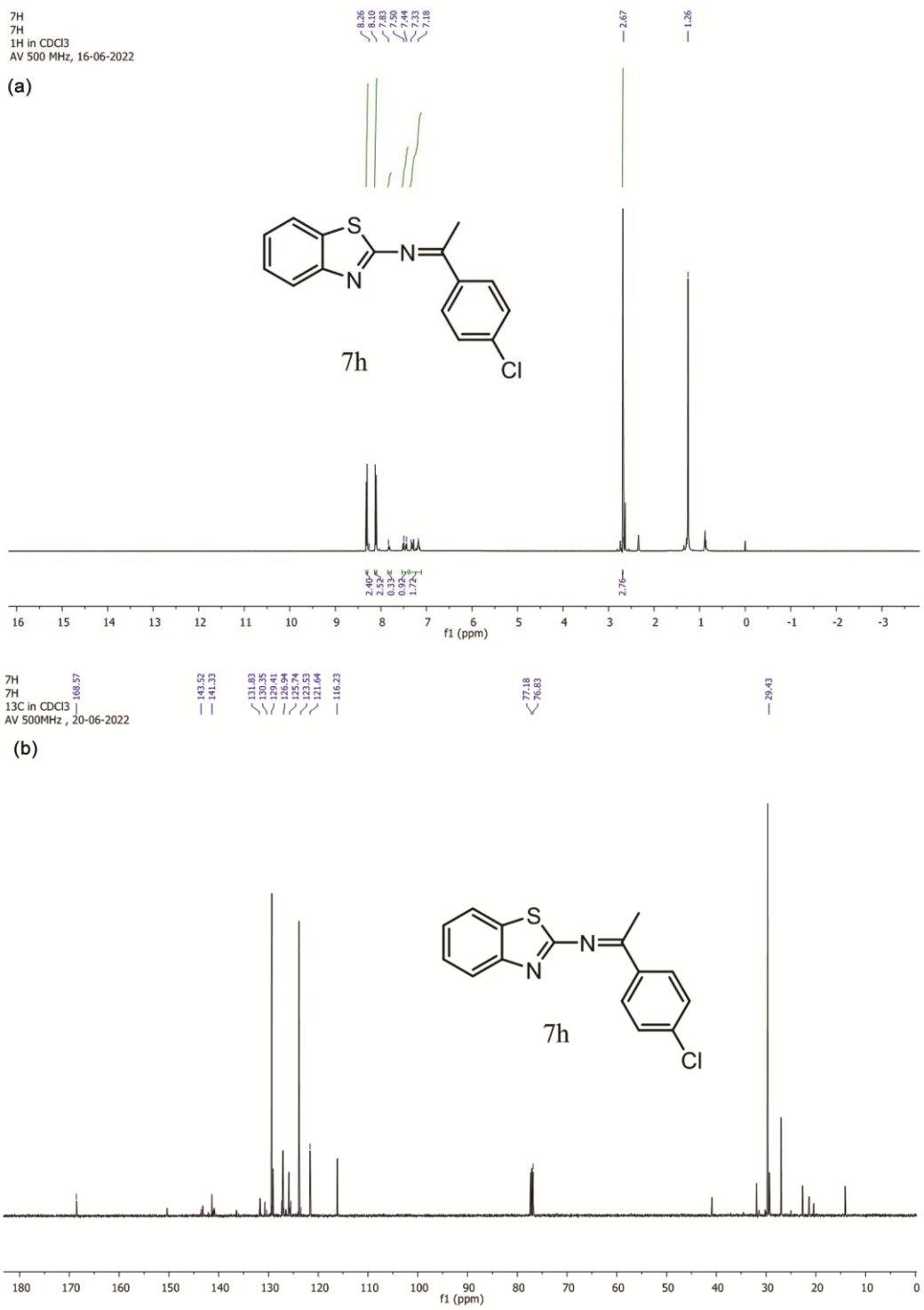

Fig. S11 — (a) ^{1}H and (b) C NMR spectra of compound 7h

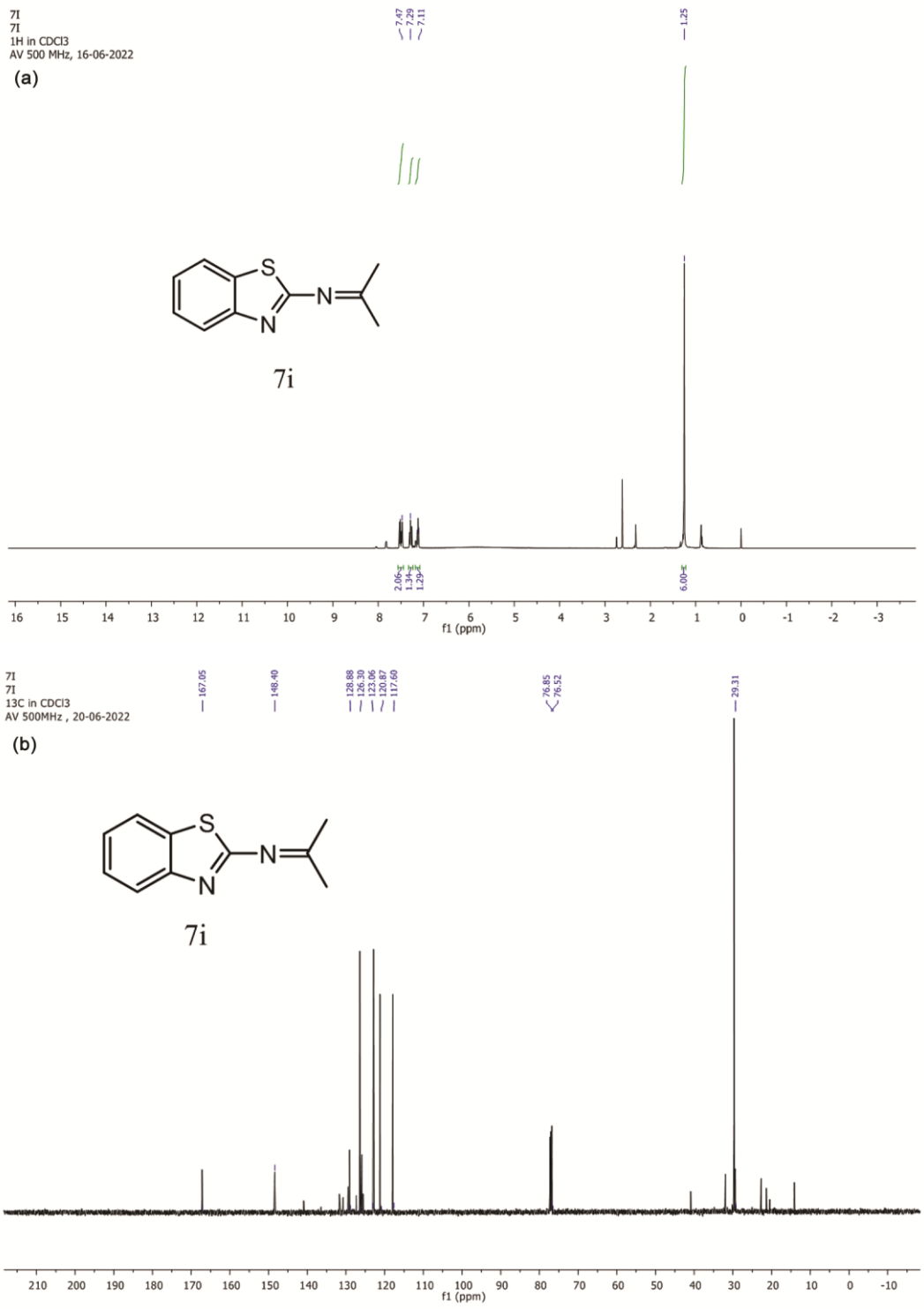

Fig. S12 — (a) ^{1}H and (b) C NMR spectra of compound 7i

Fig. S13 — (a) ^{1}H and (b) C NMR spectra of compound 7j

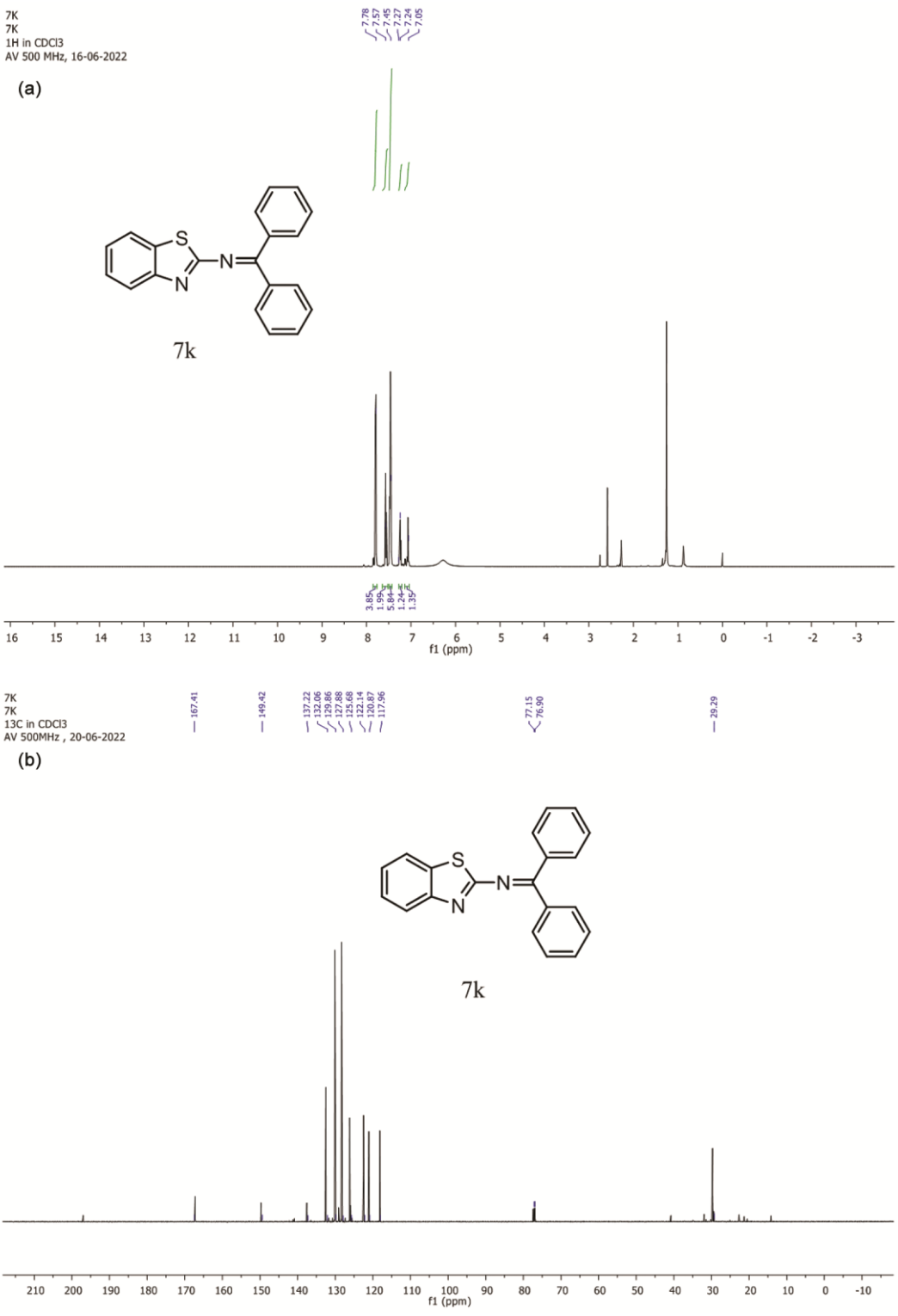

Fig. S14 — (a) ^{1}H and (b) C NMR spectra of compound 7k

Fig. S15 — (a) ^{1}H and (b) C NMR spectra of compound 7l

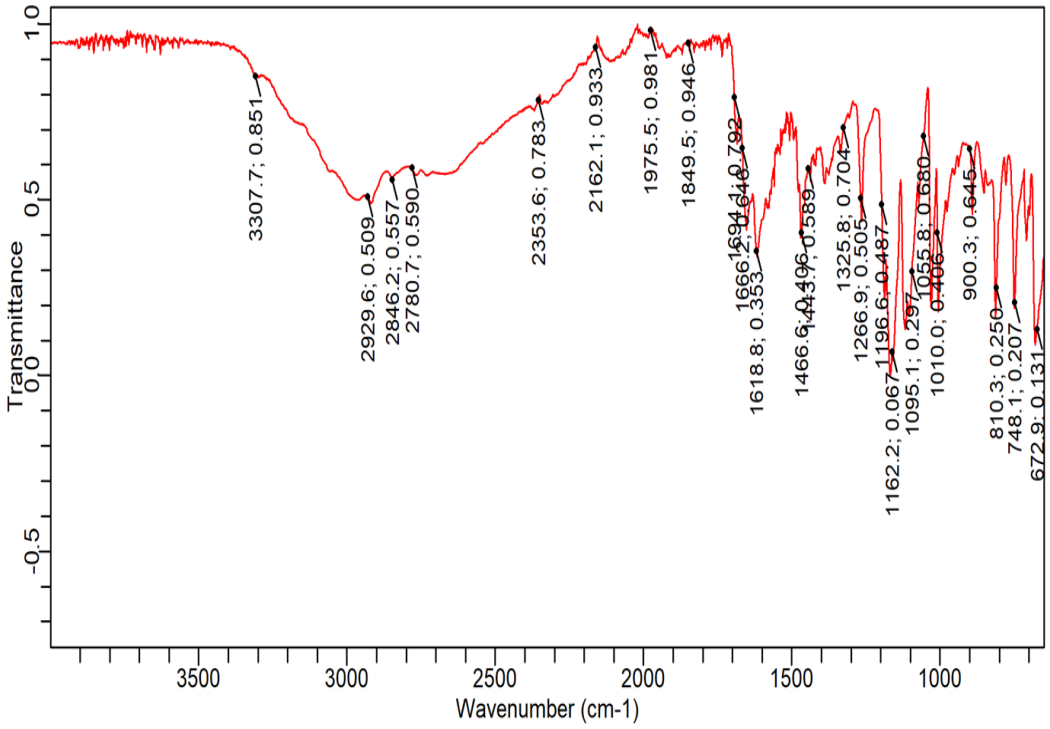
Transmittance
Wavenumber (cm-1)
3307.7; 0.851
2929.6; 0.509
2846.2; 0.557
2780.7; 0.590
2353.6; 0.783
2162.1; 0.933
1975.5; 0.981
1849.5; 0.946
1618.8; 0.353
1466.6; 0.496
1325.8; 0.704
1266.9; 0.505
1196.6; 0.487
1162.2; 0.067
1095.1; 0.297
1055.8; 0.680
1010.0; 0.406
900.3; 0.645
810.3; 0.250
748.1; 0.207
672.9; 0.131

7a

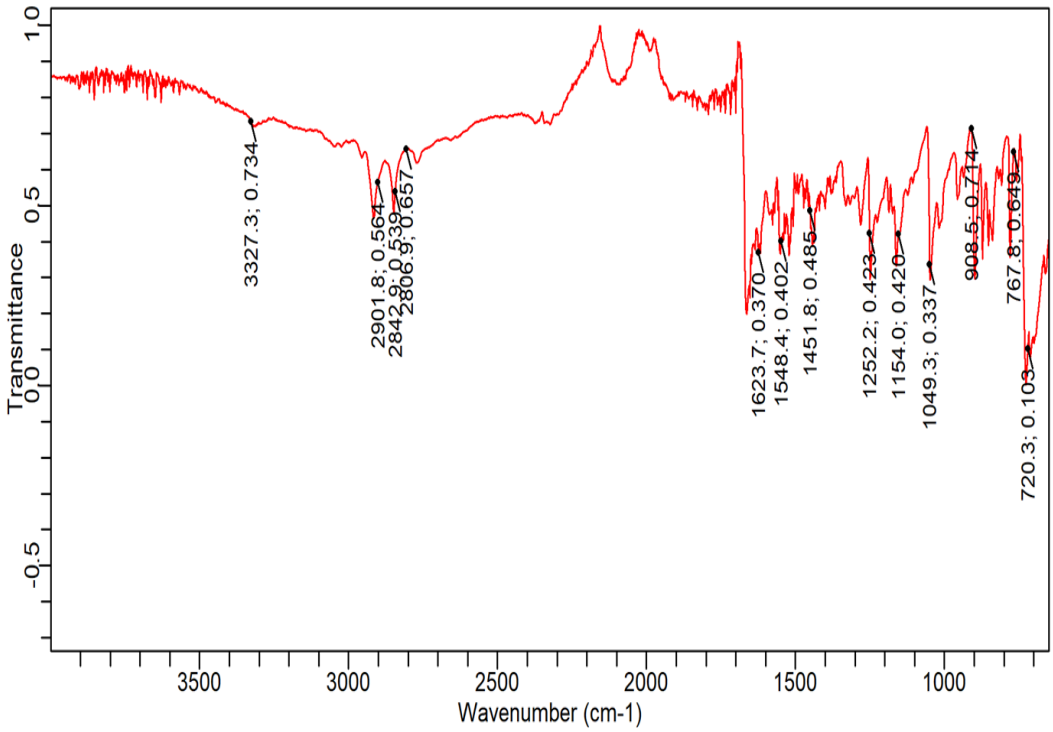
Transmittance
Wavenumber (cm-1)
3327.3; 0.734
2901.8; 0.564
2842.9; 0.539
2806.9; 0.657
1623.7; 0.370
1548.4; 0.402
1451.8; 0.485
1252.2; 0.423
1154.0; 0.420
1049.3; 0.337
908.5; 0.714
767.8; 0.649
720.3; 0.103

7b

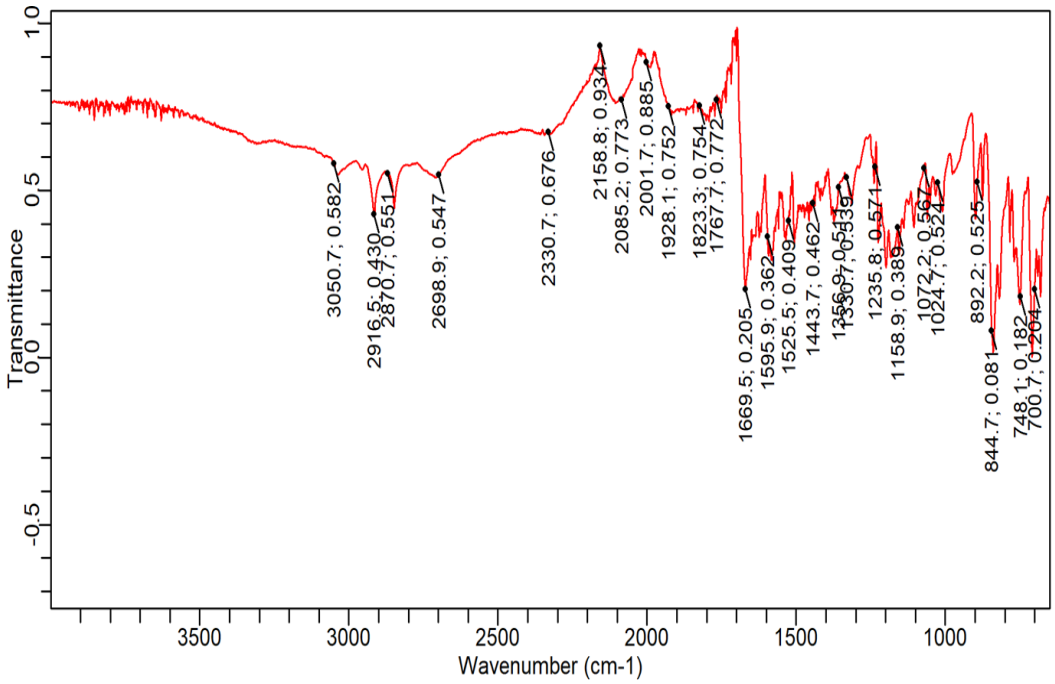
Transmittance
1.0
0.5
0.0
-0.5
3500
3000
2500
2000
1500
1000
Wavenumber (cm-1)
3050.7; 0.582
2916.5; 0.430
2870.7; 0.551
2698.9; 0.547
2330.7; 0.676
2158.8; 0.934
2085.2; 0.773
2001.7; 0.885
1928.1; 0.752
1823.3; 0.754
1767.7; 0.772
1669.5; 0.205
1595.9; 0.362
1525.5; 0.409
1443.7; 0.462
1330.7; 0.539
1235.8; 0.571
1158.9; 0.385
1072.2; 0.567
1024.7; 0.524
892.2; 0.525
844.7; 0.081
748.1; 0.182
700.7; 0.204

7c

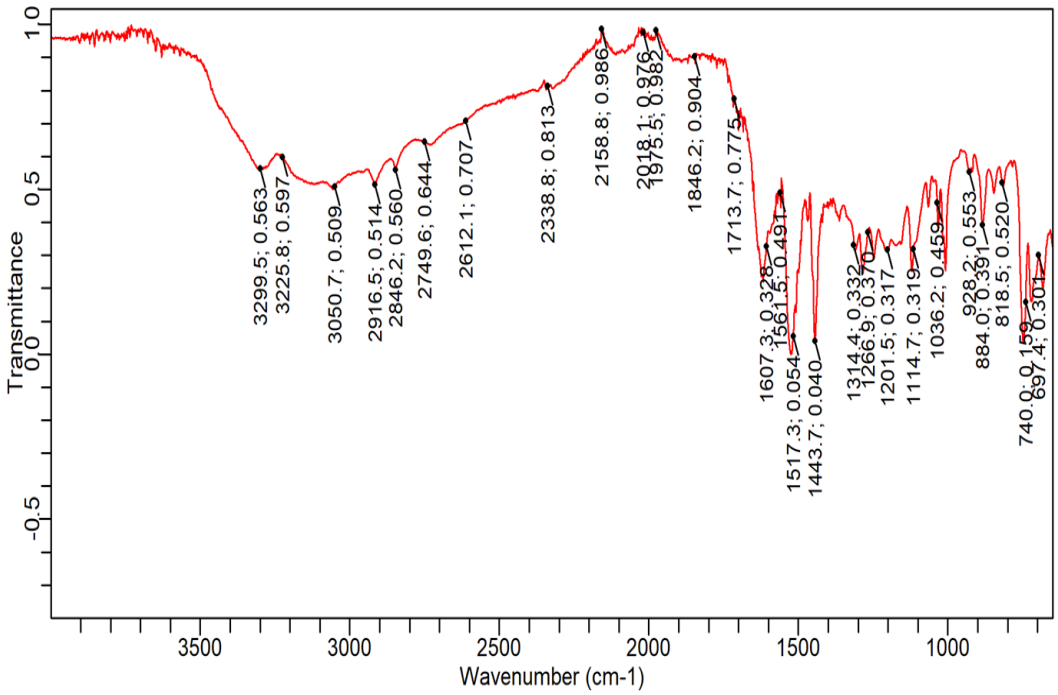
Transmittance
1.0
0.5
0.0
-0.5
3500
3000
2500
2000
1500
1000
Wavenumber (cm-1)
3299.5; 0.563
3225.8; 0.597
3050.7; 0.509
2916.5; 0.514
2846.2; 0.560
2749.6; 0.644
2612.1; 0.707
2338.8; 0.813
2158.8; 0.986
2018.1; 0.976
1975.5; 0.982
1846.2; 0.904
1713.7; 0.775
1607.3; 0.328
1561.5; 0.491
1517.3; 0.054
1443.7; 0.040
1314.4; 0.332
1266.9; 0.370
1201.5; 0.317
1114.7; 0.319
1036.2; 0.459
928.2; 0.553
884.0; 0.391
818.5; 0.520
740.0; 0.159
697.4; 0.301

7d

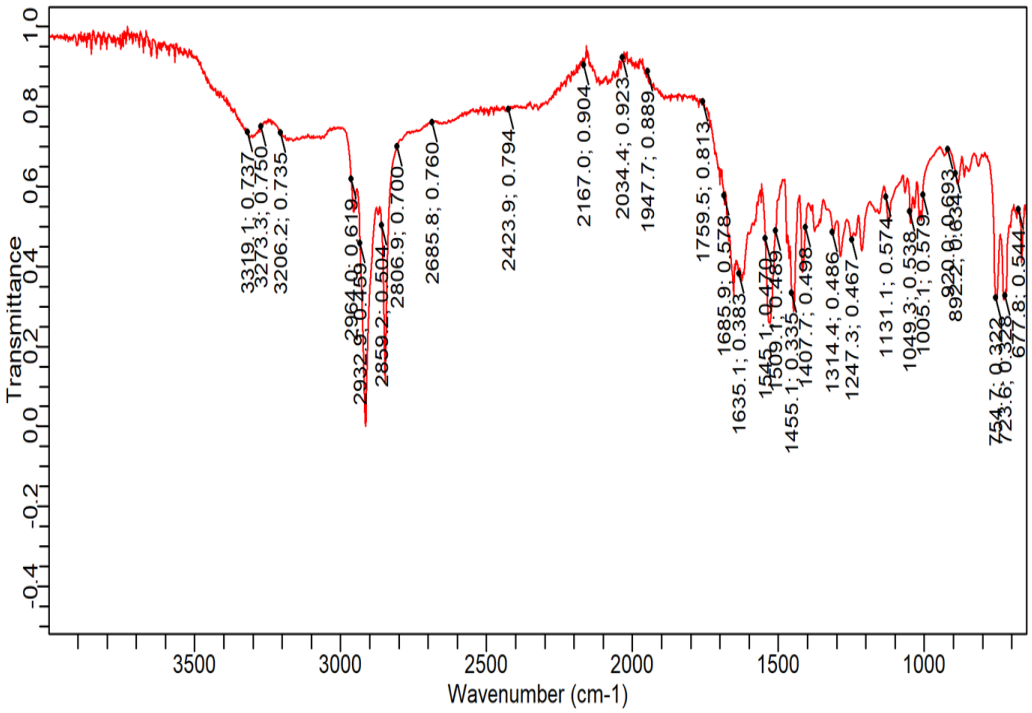
Transmittance
Wavenumber (cm-1)
3319.1; 0.737
3273.3; 0.750
3206.2; 0.735
2964.0; 0.619
2932.8; 0.469
2859.2; 0.504
2806.9; 0.700
2685.8; 0.760
2423.9; 0.794
2167.0; 0.904
2034.4; 0.923
1947.7; 0.889
1759.5; 0.813
1685.9; 0.578
1635.1; 0.383
1545.1; 0.470
1509.1; 0.485
1455.1; 0.335
1407.7; 0.498
1314.4; 0.486
1247.3; 0.467
1131.1; 0.574
1049.3; 0.538
1005.1; 0.579
892.2; 0.693
754.7; 0.322
723.6; 0.328
677.8; 0.544

7e

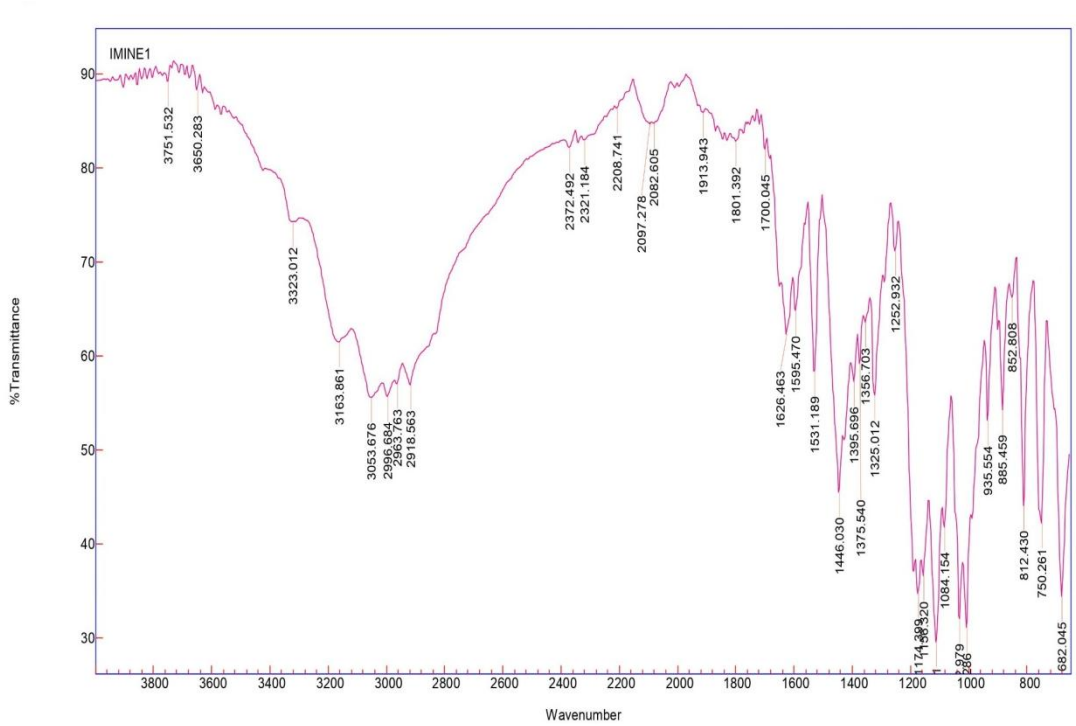
IMINE1
%Transmittance
Wavenumber
3751.532
3650.283
3323.012
3163.861
3053.676
2996.684
2963.763
2918.563
2372.492
2321.184
2208.741
2097.278
2082.605
1913.943
1801.392
1700.045
1626.463
1595.470
1531.189
1446.030
1395.696
1375.540
1356.703
1325.012
1252.932
1084.154
935.554
885.459
852.808
812.430
750.261
682.045

7f

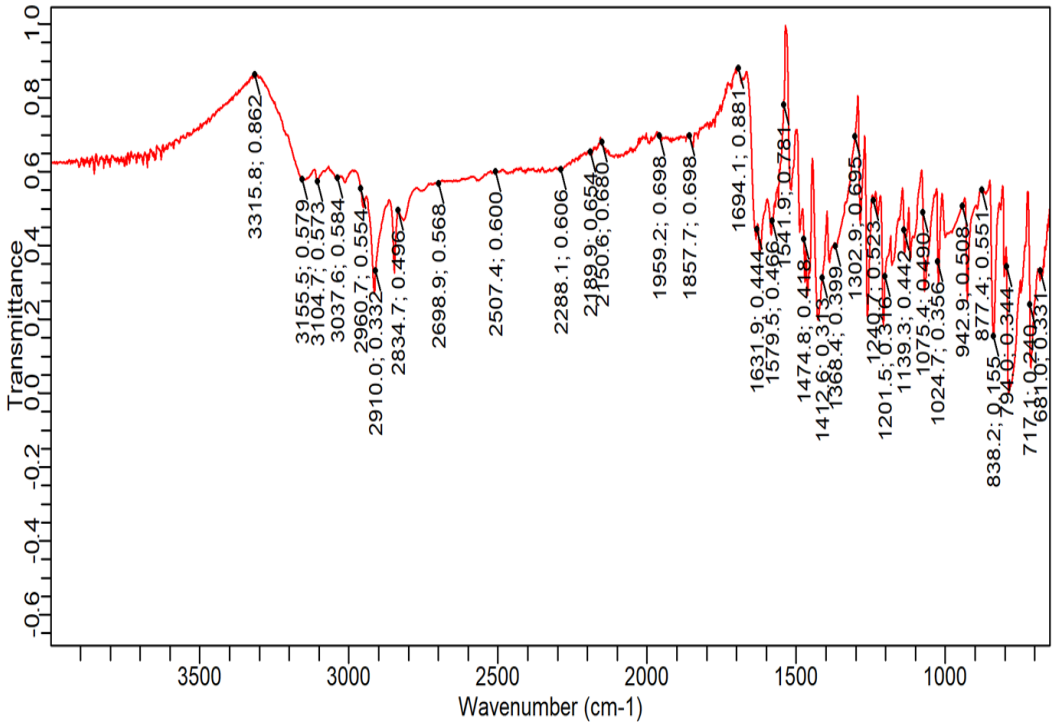
Transmittance
Wavenumber (cm-1)
3315.8; 0.862
3155.5; 0.579
3104.7; 0.573
3037.6; 0.584
2960.7; 0.554
2910.0; 0.332
2834.7; 0.496
2698.9; 0.568
2507.4; 0.600
2288.1; 0.606
2189.9; 0.654
2150.6; 0.680
1959.2; 0.698
1857.7; 0.698
1694.1; 0.881
1631.9; 0.444
1579.5; 0.466
1541.9; 0.781
1474.8; 0.418
1412.6; 0.313
1368.4; 0.399
1302.9; 0.695
1240.7; 0.523
1201.5; 0.316
1139.3; 0.442
1075.4; 0.490
1024.7; 0.356
942.9; 0.508
877.4; 0.551
838.2; 0.155
794.0; 0.344
717.1; 0.240
681.0; 0.331

7g

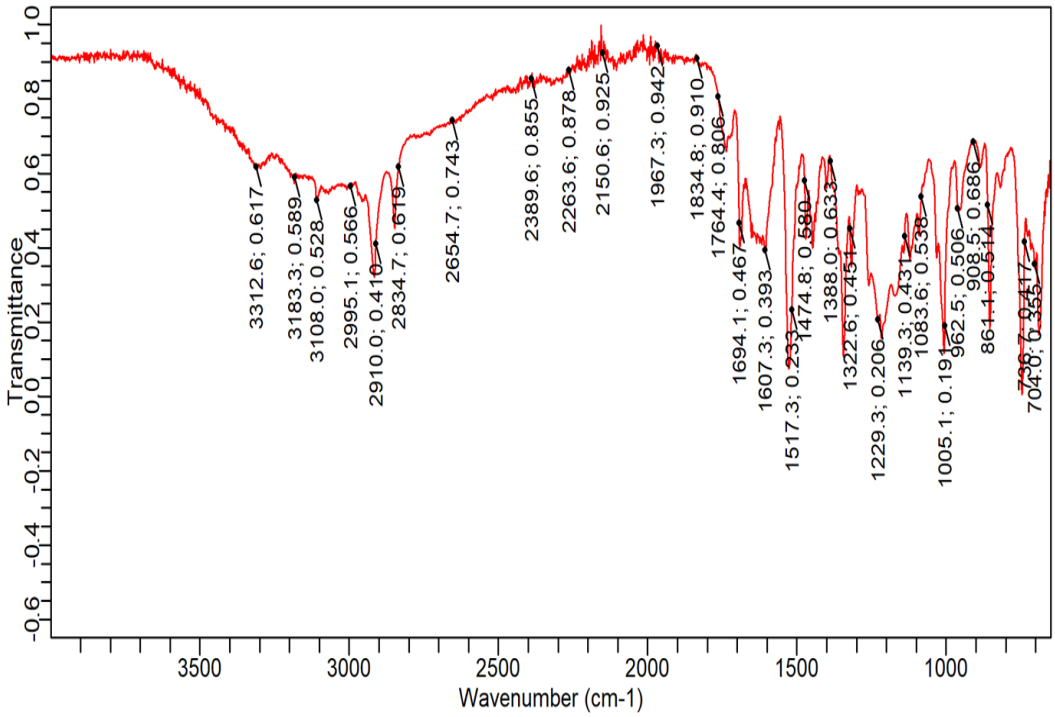
Transmittance
Wavenumber (cm-1)
3312.6; 0.617
3183.3; 0.589
3108.0; 0.528
2995.1; 0.566
2910.0; 0.410
2834.7; 0.619
2654.7; 0.743
2389.6; 0.855
2263.6; 0.878
2150.6; 0.925
1967.3; 0.942
1834.8; 0.910
1764.4; 0.806
1694.1; 0.467
1607.3; 0.393
1517.3; 0.233
1474.8; 0.580
1388.0; 0.633
1322.6; 0.451
1229.3; 0.206
1139.3; 0.431
1083.6; 0.538
1005.1; 0.191
962.5; 0.506
908.5; 0.686
861.1; 0.514
736.7; 0.417
704.0; 0.355

7h

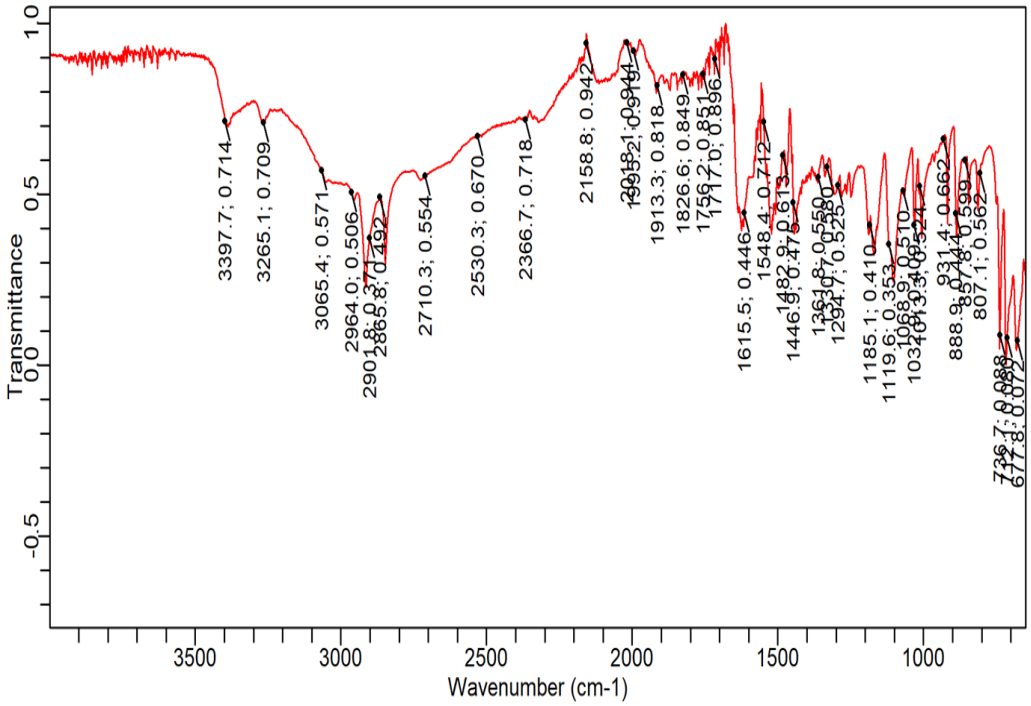
Transmittance
Wavenumber (cm-1)
3397.7; 0.714
3265.1; 0.709
3065.4; 0.571
2964.0; 0.506
2530.3; 0.670
2366.7; 0.718
2158.8; 0.942
1615.5; 0.446
1548.4; 0.712
1185.1; 0.410
807.1; 0.562

7i

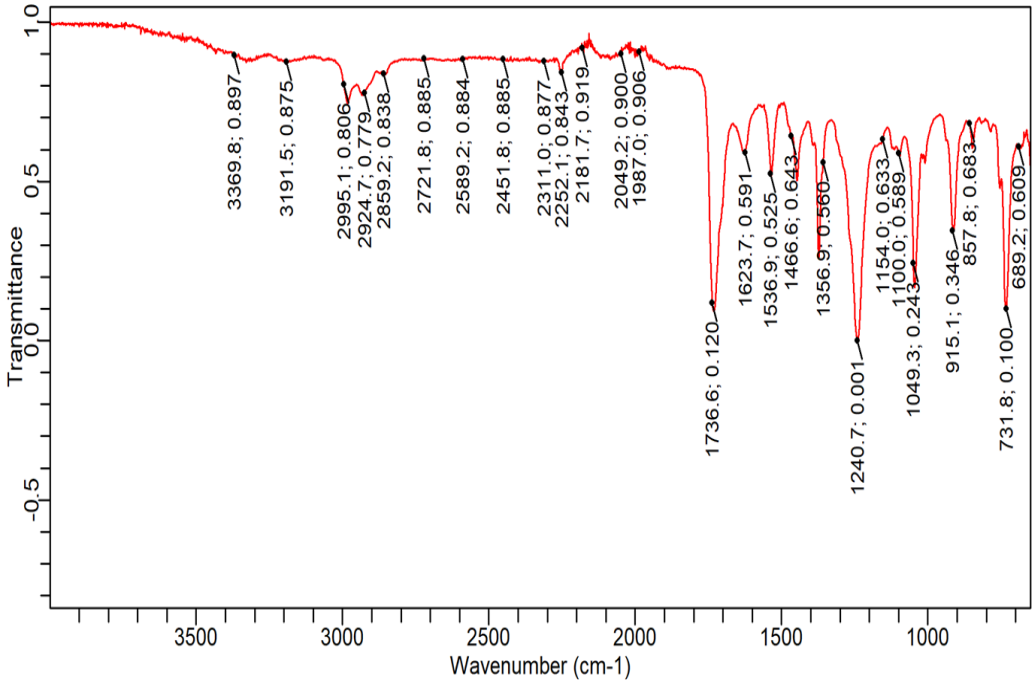
Transmittance
Wavenumber (cm-1)
3369.8; 0.897
3191.5; 0.875
2995.1; 0.806
2924.7; 0.779
2859.2; 0.838
2721.8; 0.885
2589.2; 0.884
2451.8; 0.885
2311.0; 0.877
2252.1; 0.843
2181.7; 0.919
2049.2; 0.900
1987.0; 0.906
1736.6; 0.120
1623.7; 0.591
1536.9; 0.525
1466.6; 0.643
1356.9; 0.560
1240.7; 0.001
1154.0; 0.633
1100.0; 0.589
1049.3; 0.243
915.1; 0.346
857.8; 0.683
731.8; 0.100
689.2; 0.609

7j

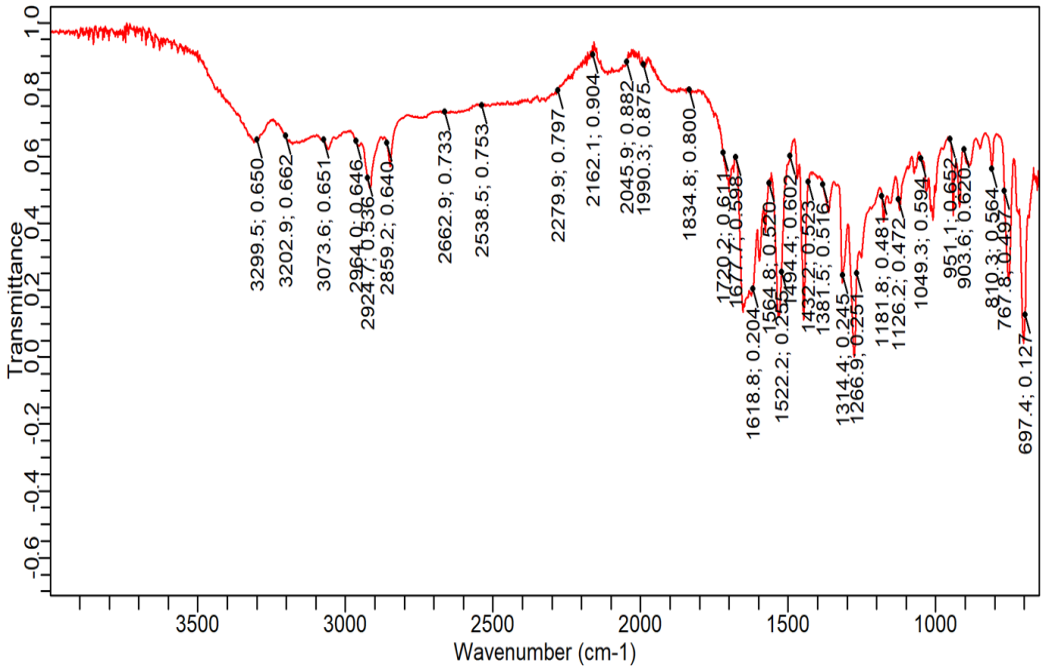

7k

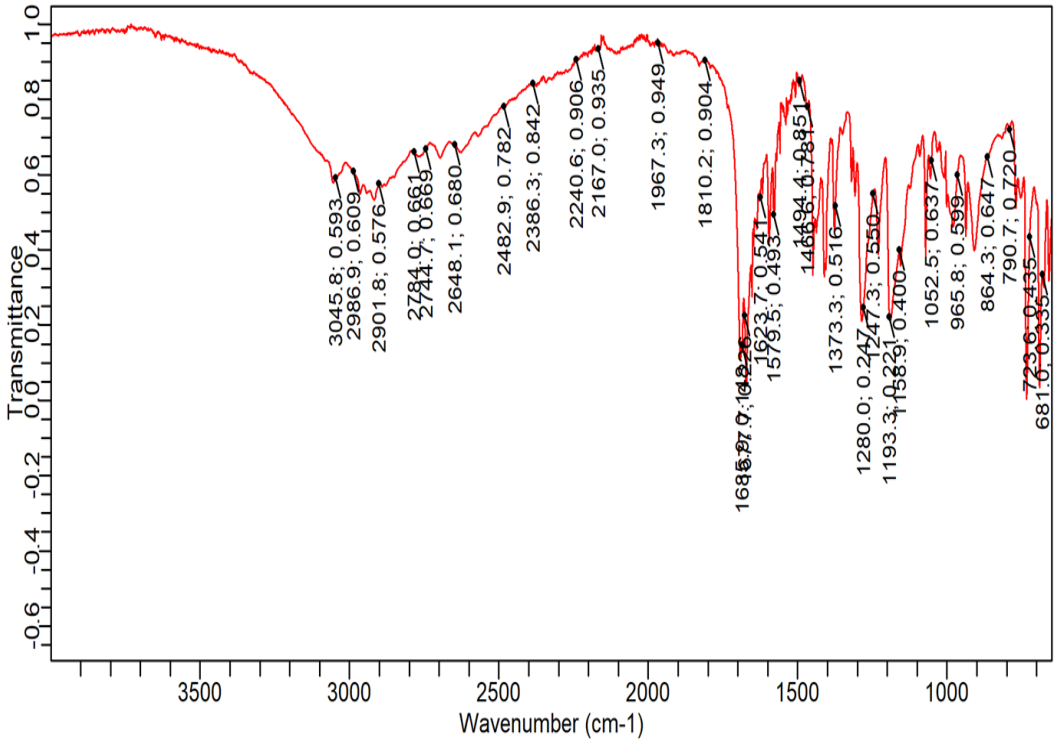

7l

Fig. S16 — FTIR spectra of compound 7a-l